

# Solvent Effects on the Actinic Step of Donor–Acceptor Stenhouse Adduct Photoswitching

Michael M. Lerch<sup>+</sup>, Mariangela Di Donato<sup>+</sup>, Adèle D. Laurent, Miroslav Medved<sup>†</sup>, Alessandro Iagatti, Laura Bussotti, Andrea Lapini, Wybren Jan Buma, Paolo Foggi, Wiktor Szymański,\* and Ben L. Feringa\*

**Abstract:** Donor–acceptor Stenhouse adducts (DASAs) are negative photochromes that switch with visible light and are highly promising for applications ranging from smart materials to biological systems. However, the strong solvent dependence of the photoswitching kinetics limits their application. The nature of the photoswitching mechanism in different solvents is key for addressing the solvatochromism of DASAs, but as yet has remained elusive. Here, we employ spectroscopic analyses and TD-DFT calculations to reveal changing solvatochromic shifts and energies of the species involved in DASA photoswitching. Time-resolved visible pump-probe spectroscopy suggests that the primary photochemical step remains the same, irrespective of the polarity and protic nature of the solvent. Disentangling the different factors determining the solvent-dependence of DASA photoswitching, presented here, is crucial for the rational development of applications in a wide range of different media.

Molecular photoswitches change structure and properties reversibly upon light-irradiation,<sup>[1]</sup> enabling successful applications in the dynamic control of functions in material sciences,<sup>[2–4]</sup> supramolecular chemistry,<sup>[5,6]</sup> and in the biological context.<sup>[7–12]</sup> Applications differ markedly in the environment the photoswitch is exposed to, be it different solvents,<sup>[13,14]</sup> matrices or surfaces, and understanding how

a given photoswitch behaves in various environments is crucial for its success in any applications.

Donor–acceptor Stenhouse adducts (DASAs, Figure 1 a) were introduced in 2014<sup>[17,18]</sup> and feature important advantages as compared to traditional photoswitches, including visible light responsiveness<sup>[11,19,20]</sup> and negative photochromism.<sup>[21]</sup> Moreover, their modular architecture<sup>[22]</sup> allows for a fine-tuning of properties.<sup>[23]</sup> First-generation DASAs (**1** and **2**, Figure 1 a)<sup>[17,18]</sup> are based on dialkylamine donors, whereas second-generation DASAs (**3**)<sup>[24,25]</sup> employ secondary anilines leading to bathochromically shifted spectra. Upon irradiation in toluene, the strongly colored elongated DASA (**A**) cyclizes to a colorless form (**B**) that then thermally opens back to the triene form (**A**). First-generation DASAs switch reversibly only in aromatic solvents such as toluene. In water and methanol, in contrast, irreversible cyclization takes place. In chlorinated solvents, photo-isomerization (to form **A'**, Figure 1 b) is observed, but it is not followed by cyclization.<sup>[15,16,18]</sup> Second-generation DASAs, however, do cyclize in chlorinated solvents.

A clear understanding of the photoswitching mechanism is key to disentangle the influence of solvents on the observed photoswitching behavior (Figure 1 b). Our current mechanistic hypothesis suggests an initial photoisomerization around C<sub>2</sub>–C<sub>3</sub>, followed by a rotation around C<sub>3</sub>–C<sub>4</sub>, to facilitate

[\*] M. M. Lerch,<sup>[‡]</sup> Dr. W. Szymański, Prof. Dr. B. L. Feringa  
Centre for Systems Chemistry, Stratingh Institute for Chemistry  
University of Groningen  
Nijenborgh 4, 9747 AG, Groningen (The Netherlands)  
E-mail: w.c.szymanski@rug.nl  
b.l.feringa@rug.nl

Dr. W. Szymański  
Department of Radiology, University of Groningen  
University Medical Center Groningen  
Hanzeplein 1, 9713 GZ, Groningen (The Netherlands)  
E-mail: w.c.szymanski@umcg.nl

Dr. M. D. Donato,<sup>[‡]</sup> Dr. A. Iagatti, Dr. L. Bussotti, Dr. A. Lapini,  
Prof. Dr. P. Foggi  
European Laboratory for Non Linear Spectroscopy (LENS)  
via N. Carrara 1, 50019 Sesto Fiorentino (Italy)

Dr. M. D. Donato,<sup>[‡]</sup> Dr. A. Iagatti, Dr. A. Lapini, Prof. Dr. P. Foggi  
Istituto Nazionale di Ottica  
Largo Fermi 6, 50125 Firenze (Italy)  
Prof. Dr. P. Foggi  
Dipartimento di Chimica, Università di Perugia  
via Elce di Sotto 8, 06100 Perugia (Italy)

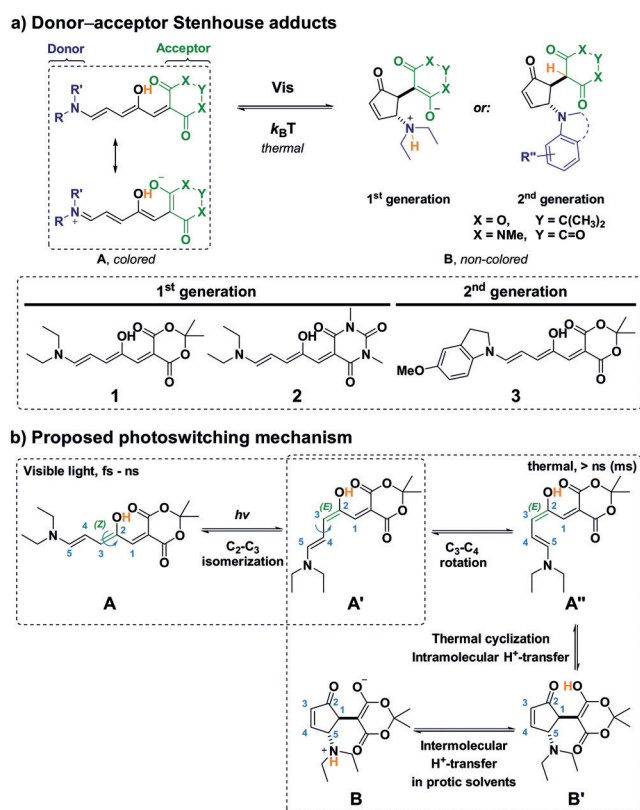
Dr. A. D. Laurent  
CEISAM, UMR CNRS 6230, BP 92208  
2 Rue de la Houssinière, 44322 Nantes, Cedex 3 (France)

Dr. M. Medved<sup>†</sup>  
Regional Centre of Advanced Technologies and Materials, Department of Physical Chemistry, Faculty of Science  
Palacký University in Olomouc  
17. listopadu 1192/12, CZ-771 46 Olomouc (Czech Republic)  
Dr. M. Medved<sup>†</sup>  
Department of Chemistry, Faculty of Natural Sciences  
Matej Bel University  
Tajovského 40, SK-97400 Banská Bystrica (Slovak Republic)  
Prof. Dr. W. J. Buma  
Van't Hoff Institute for Molecular Sciences, University of Amsterdam  
Science Park 904, 1098XH Amsterdam (The Netherlands)

[†] These authors contributed equally.

Supporting information and the ORCID identification number(s) for the author(s) of this article can be found under:  
<https://doi.org/10.1002/anie.201803058>.

© 2018 The Authors. Published by Wiley-VCH Verlag GmbH & Co. KGaA. This is an open access article under the terms of the Creative Commons Attribution-NonCommercial-NoDerivs License, which permits use and distribution in any medium, provided the original work is properly cited, the use is non-commercial and no modifications or adaptations are made.



**c) Energy level diagram for 1 in selected solvents**

**Figure 1.** Donor-acceptor Stenhouse adducts: a) photoswitches used herein; b) proposed photoswitching mechanism<sup>[15,16]</sup> and c) corresponding energy level diagram in kcal mol<sup>-1</sup> for 1 in selected solvents obtained at the M06-2X/6-31+G(d)/SMD level of theory. Analogous diagrams for 2 and 3 are presented in the SI (Figure S8.5). In the electronic density difference (EDD) plot (inset), the blue (red) regions correspond to a decrease (increase) in electron density upon electronic excitation. The energy levels of the product correspond to B and B' structures in protic and aprotic solvents, respectively.

a subsequent thermal cyclization accompanied with proton transfer (Figure 1b).<sup>[16]</sup> Bieske and co-workers recently showed the possibility to drive the thermal steps in the gas phase by additional light-absorption.<sup>[26]</sup> Earlier, observation of a transient absorption band in toluene under steady state conditions for first-generation DASAs was attributed to the product of the actinic step A' (Figure 1b and 2c).<sup>[15]</sup> Importantly however, such a transient absorption band cannot be

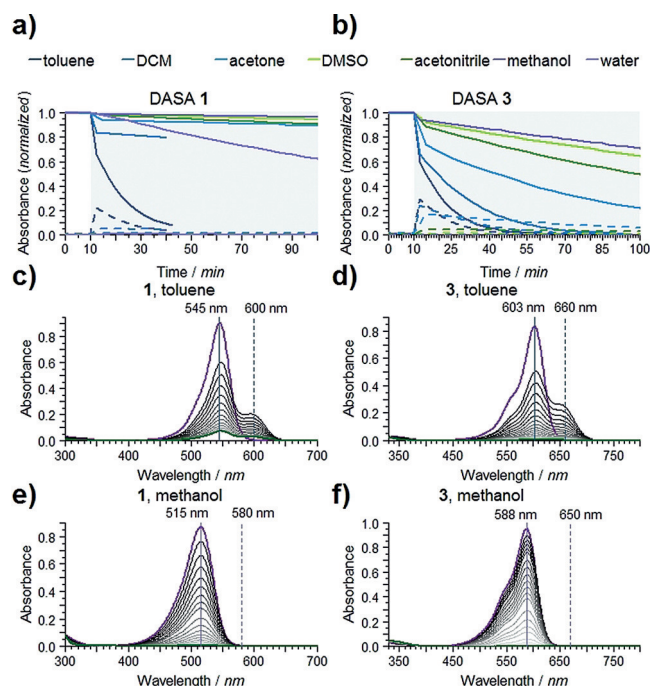


**Figure 2.** Solvent effects on DASA photoswitching for compound 1 (a) and 3 (b). Absorption spectra manifesting the photoswitching process of compound 1 and 3 in toluene (c and d) and methanol (e and f).

detected in polar protic solvents (e.g., methanol and water, Figure 2e) under steady-state conditions where photoswitching is slowed down by at least two orders of magnitude (Figure 2; Supporting Information (SI) section 5 and 6) and proceeds, albeit slowly, even without irradiation (SI section 3). These observations raise questions about the nature of the photoswitching mechanism in various solvents.

We set out to study the actinic step of 1–3 using ultrafast time-resolved spectroscopy<sup>[27,28]</sup> across a range of solvents, in order to verify if the nature of the intermediate species formed upon light absorption remains the same. We further tried to understand why photoswitching is reversible only in selected solvents and which factors determine the observed large differences in photoswitching kinetics. Here, we provide evidence that DASAs undergo the same actinic step irrespective of the solvent used. DFT calculations unveil the overall kinetics and thermodynamics governing the reversibility of photoswitching (Figure 1c). Furthermore, solvents influence the band-overlap of A and A', potentially influencing the photostationary states reached and thus affecting overall cyclization kinetics.

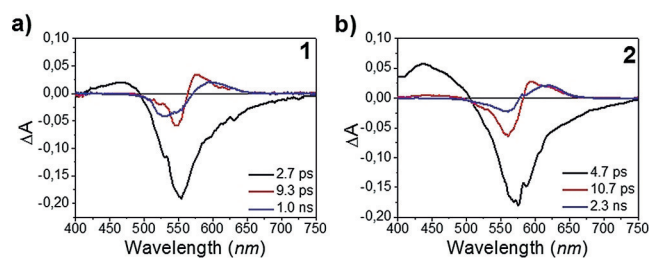


**Figure 3.** Evolution-associated difference spectra (EADS) obtained by global analysis<sup>[29]</sup> of compound 1 and 2 in toluene.

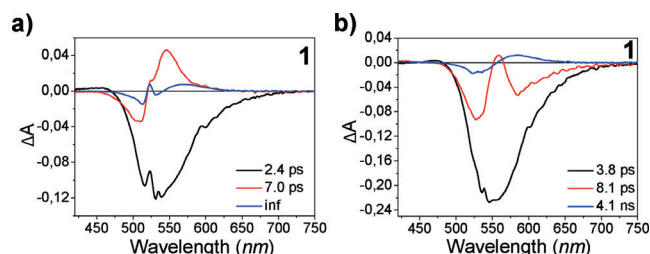
**Table 1:** EADS<sup>[29]</sup> associated lifetimes for the photo-isomerization and its quantum yield for compound 1–3 in different solvents.

#	Solvent	Compound 1			Compound 2			Compound 3		
		Lifetime [ps]		$\varphi_{A \rightarrow A'}$ [%]	Lifetime [ps]		$\varphi_{A \rightarrow A'}$ [%]	Lifetime [ps]		$\varphi_{A \rightarrow A'}$ [%]
		$\tau_1$	$\tau_2$		$\tau_1$	$\tau_2$		$\tau_1$	$\tau_2$	
1	Toluene	2.7	9.3	21.0	4.7	10.7	10.6	1.0	23.8	14.5
2	Dichloromethane	2.1 <sup>[16]</sup>	6.1 <sup>[16]</sup>	10.8	4.4	10.3	14.3	2.1 <sup>[16]</sup>	25.9 <sup>[16]</sup>	9.3
3	Methanol	2.4	7.0	12.4	4.0	7.6	10.8	1.5	20.6	16.0
4	Dimethylsulfoxide	3.8	8.1	8.3	3.0	11.8	9.5	2.5	62.3	10.1

Figure 3 reports the EADS (evolution-associated difference spectra) obtained by global analysis<sup>[29]</sup> of ultrafast visible pump-probe data recorded for compounds **1** and **2** in toluene (for other solvents see SI section 7 and Table 1). Upon excitation, the bleaching of the ground state population is observed as an intense negative band ( $\lambda_{\max} = 554$  nm for **1** and  $\lambda_{\max} = 574$  nm for **2**). A low-intensity excited state absorption band is visible in the first EADS (black EADS in Figure 3), peaking at 466 nm and 437 nm for **1** and **2**, respectively. In the case of **1**, the intensity of the bleaching band recovers by more than half in about 2.7 ps and on the same timescale an absorption band peaking at about 575 nm develops (red EADS in Figure 3). For DASA **2**, this happens within 4.7 ps and leads to a band at  $\lambda_{\max} = 594$  nm. On a 9.3 (10.7) ps timescale for **1** (**2**), the intermediate absorption band slightly red-shifts while its intensity decreases (blue EADS in Figure 3,  $\lambda_{\max} = 596$  nm for **1** and  $\lambda_{\max} = 619$  nm for **2**). Despite the difference in the acceptor moiety that affects the  $A \rightarrow A^*$  transition, the kinetics of the actinic step are comparable. In fact, only a slight increase in both the first and second lifetimes is observed for the barbituric system, which contrasts with the overall faster photoswitching of **2** as compared to **1**.<sup>[17]</sup> A target analysis<sup>[29]</sup> of the transient absorption data recorded in chloroform suggested that the broad positive band in the red EADS (Figure 3) results from the combined absorption of two species, originating from a branched decay of  $A^*$  into both  $A'$  and the hot ground state of  $A$ .<sup>[16]</sup> Table 1 reports the time constants describing the kinetics of the photoinduced isomerization for both compounds and an estimation of the quantum yield for the process, showing that even though the investigated solvents are very different in terms of polarity, polarizability and protic nature, the observed kinetics do not differ significantly. In all cases, the absorption band associated with intermediate  $A'$ <sup>[16]</sup> is observed to rise on a few picosecond timescale. For sample **2**, a slight dependence of the kinetic traces taken at the maximum of the intermediate absorption on solvent polarity is observed (Figure S7.6), which is barely noted in the case of sample **1** (Figure S7.3).

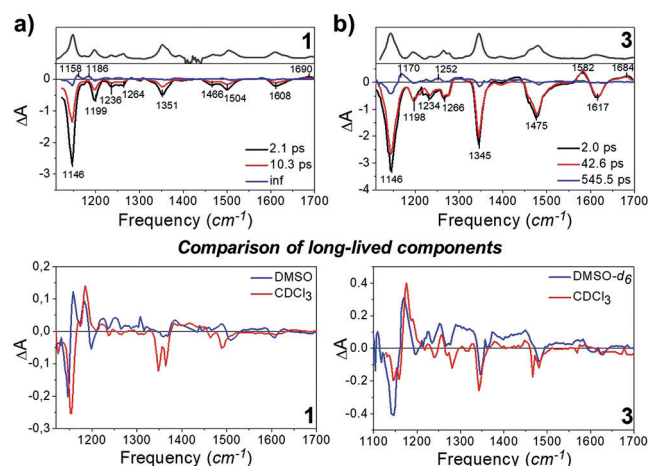
The behavior of second-generation DASA **3** in different solvents follows closely the previously described behavior in chloroform<sup>[16]</sup> (Table 1, Figure S7.7–S7.9). The major difference with first-generation DASAs is that the excited state of the elongated form lives long enough to allow cooling to occur in the excited state before isomerization. As a result, the red shift of the positive band rising on the ps timescale is not observed since the hot ground state of  $A$  is not involved in the relaxation process. Solvent effects on the isomerization

kinetics are generally minor, except in dimethyl sulfoxide (DMSO), where the photoisomerization rates decrease for all the analyzed compounds and more markedly for compound **3**. Notably, this is also the case when the viscosity of the solvent is increased (as for instance can be achieved

**Figure 4.** Transient absorption spectra of DASA **1** in methanol (a) and dimethyl sulfoxide (b) showing the influence of viscosity on the decay dynamics.

with a 60/40 wt % glycerol/methanol mixture, SI section 7). Figure 4 shows that increasing the viscosity leads to a slower in-growth of the positive absorption band attributed to the intermediate (see raw data reported in SI section 7). As a result, the absorption band of the intermediate appears in dimethyl sulfoxide (Figure 4b) as a structuring of the bleaching feature instead of a positive absorption band as observed in methanol (Figure 4a).

Analysis of time-resolved infrared (TRIR) spectra (Figure 5) and comparison of experimental and computed difference spectra of the possible photogenerated isomers (Figure 6) provides additional information on the structure of the intermediate  $A'$  in different solvents. The comparison of

**Figure 5.** Comparison of EADS obtained by global analysis<sup>[29]</sup> of TRIR data for a) DASA **1** in DMSO and b) DASA **3** in  $[D_6]$ DMSO. The upper traces in these two panels display steady-state FTIR spectra of the two compounds. In panels c) and d), a comparison is shown between the long-lived components in DMSO/ $[D_6]$ DMSO and deuterated chloroform.<sup>[16]</sup>



the long-lived spectral component of **1** and **3** in different solvents (Figure 5c and 5d, respectively), which represents the  $A' - A$  difference spectrum, shows that the IR spectrum of compound **3** is barely influenced by the solvent, while a few differences can be noticed for compound **1**, particularly in the C–C stretching and C–H rocking region ( $1100\text{--}1200\text{ cm}^{-1}$ ). This is also noticeable for their corresponding FTIR spectra (Figure S2.1 and S2.2, SI section 2). Nevertheless, the comparison between experimental and computed difference IR spectra (see below) suggests that the light induced photoisomerization remains the same in all investigated solvents, and that small changes in the EADS shapes are caused by solvatochromic shifts of the IR absorption bands.

To better understand the effects of substitution and solvent on the kinetics and thermodynamics of the photo-switching process, key steps of the proposed mechanism were studied by (TD-)DFT in combination with the implicit solvent model (SMD) (see SI section 8 for computational details). The results for **1–3** in selected solvents are summarized in Table S8.1 and illustrated in Figures 1c and S8.5. In line with experimental observations, the calculations show that the nature of the solvent strongly affects both the kinetics and thermodynamics of the photo-switching reaction. In particular,

the activation barrier for the  $C_3\text{--}C_4$  bond rotation and the product stability are significantly affected, inducing different DASA behavior after photoactivation. The irreversibility of the whole process for **1** and **2** in polar protic solvents, such as water and methanol, can be rationalized in terms of a higher thermodynamic stability of the zwitterionic form **B** compared to **A** and also by a relatively high barrier for the backward  $B \rightarrow A''$  transition. The formation of **B** through intermolecular proton transfer could further be mediated by the protic solvent. On the other hand, in aprotic solvents the cyclization step stops at the formation of a neutral form **B'** whose stability (taking the energy of **A** as zero) decreases with increasing solvent polarity. This can explain the observed reversible photoswitching in toluene, whereas in more polar, non-protic, chlorinated solvents the cyclization does not occur. Importantly, it also should be noticed that the transition barriers (for both  $A' \rightarrow A''$  and  $A'' \rightarrow B'/B$ ) are the lowest for toluene, which again supports the reversibility and relatively fast kinetics of the photoswitching in this solvent. On the contrary, the barrier for the  $C_3\text{--}C_4$  bond rotation is the highest for methanol (due to a smaller dipole moment of **TS** (5.0 D) compared to **A'** (11.3 D) as revealed by DFT computations), which explains the observed slow dynamics in this solvent.

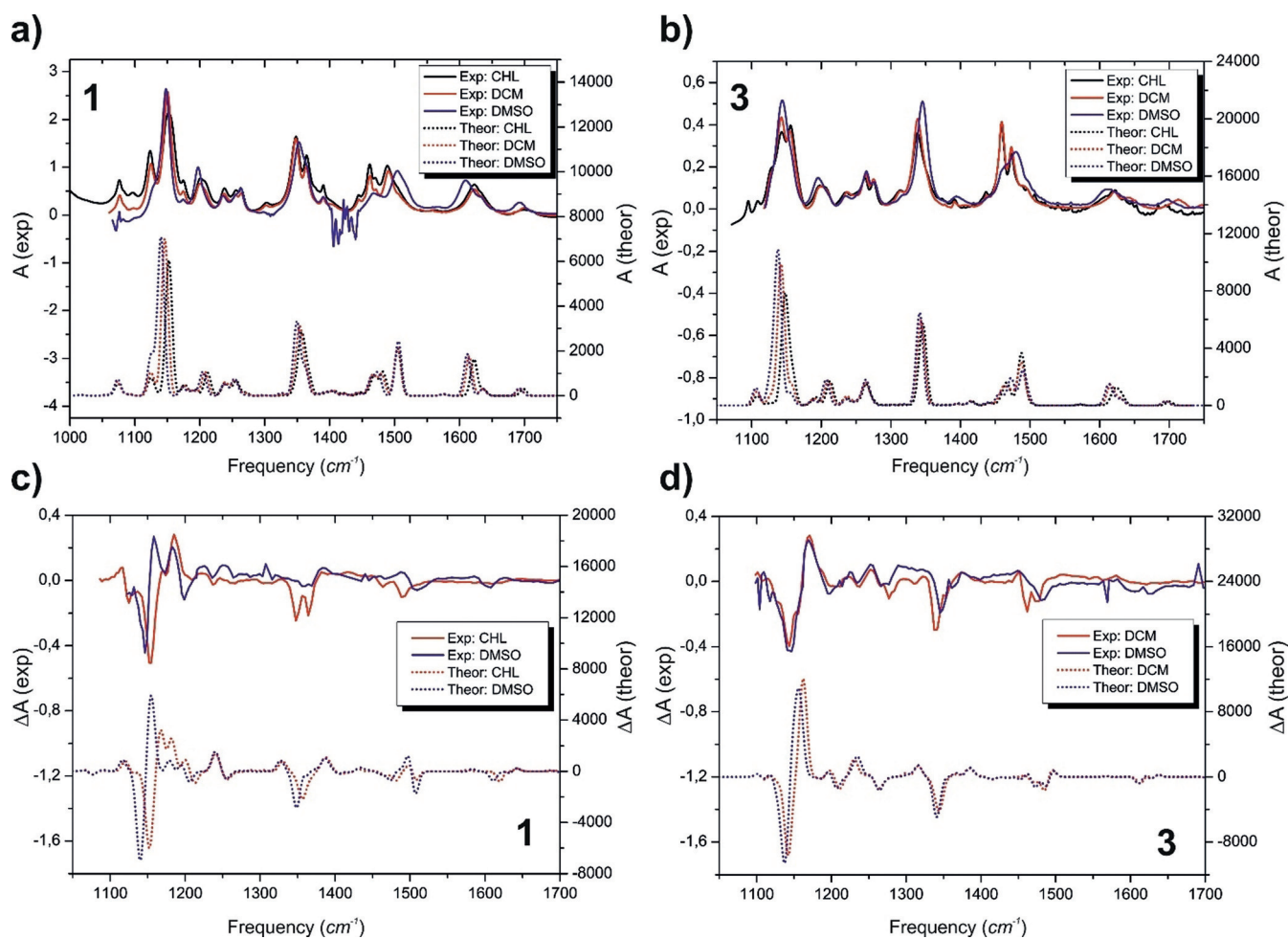


**Figure 6.** Comparison of experimental and calculated ground state IR spectra (a, b) and the long-lived component of TRIR EADS (c, d) of compounds **1** and **3** in deuterated chloroform (CHL), deuterated dichloromethane (DCM), and (deuterated) dimethyl sulfoxide (DMSO).

Whereas the  $\text{TS}(\mathbf{A}' \rightarrow \mathbf{A}'')$  parameters are comparable for **1** and **2**, the barrier is noticeably smaller (by ca. 2 kcal mol<sup>-1</sup>) for **3** (Figure S8.5 and Table S8.1).

In Figure 6 we present a comparison of experimental and simulated ground state IR spectra and the long-lived component of the TRIR EADS of compounds **1** and **3** in various solvents, the latter being constructed from the  $\mathbf{A}' - \mathbf{A}$  difference spectrum. The main features of the measured spectra are well reproduced by the DFT calculations. Notably, although the overall shapes of the ground state IR spectra of both compounds (Figures 6a and 6b) are preserved in the solvents employed, small frequency shifts and changes of peak intensities can have a large impact on the shape of IR EADS (Figures 6c and 6d). The most significant feature of the ground state IR spectra of DASAs is the band at ca. 1150 cm<sup>-1</sup> that mainly corresponds to concerted stretching vibrations of single C–C bonds coupled with C–H rocking/scissoring vibrations. Its frequency slightly decreases with increasing polarity of the solvent, which is reflected in the EADS as well. The long-lived EADS component of **3** is much less sensitive to the polarity of solvent than that of **1**, which is related to larger solvatochromic shifts for  $\mathbf{1-A}'$  compared to  $\mathbf{3-A}'$  (see Figure S8.6).

Calculations not only account for the negative DASA solvatochromism (Figures S4.1–S4.3, SI section 4),<sup>[30]</sup> but also for solvent-induced differences in the spectral shifts for  $\mathbf{A}$  and  $\mathbf{A}'$  observed in ultrafast and steady state measurements. The spectral separation of the maximum absorption of  $\mathbf{A}'$  (positive peak in the long-lived component, blue EADS) and  $\mathbf{A}$  (negative band in short-lived component, black EADS) decreases with increasing solvent polarity, with concurrent broadening of the absorption band of the elongated form  $\mathbf{A}$  in more polar protic solvents. This explains why a bathochromically shifted absorption band was not observed in previous steady-state spectroscopic measurements performed under continuous illumination.<sup>[15]</sup>

A proton-transfer—the nature of which remains elusive—is expected to be involved in the photoswitching mechanism (Figure 1b). A comparison of the transient absorption spectra of compound **1** in normal and deuterated methanol shows negligible differences in the band shape (Figure S7.16) and the associated kinetics (Figure S7.17), indicating that at the level of the actinic step solvent deuteration does not have any detectable influence, and excluding an early solvent-mediated proton-transfer.

The present data thus unambiguously demonstrate that solvents influence the thermal steps in the photoswitching mechanism but barely affect the nature of the actinic step itself. Notably, solvatochromism of  $\mathbf{A}$  and  $\mathbf{A}'$ , altering their band-overlap, suggests that the photostationary state of  $\mathbf{A}'$  reached under irradiation could govern the overall photoswitching rate. In polar protic solvents, where the  $\mathbf{A}$  and  $\mathbf{A}'$  bands overlap strongly, a lower steady-state concentration of  $\mathbf{A}'$  is expected, since this species can be switched back to the elongated form upon irradiation at the same wavelength used to isomerize  $\mathbf{A}$ . Together with the increased stabilization of the zwitterionic, colorless cyclized form  $\mathbf{B}$  in such media, these effects account for the observed slow and irreversible photoswitching of DASAs.

In conclusion, although solvents strongly influence the overall photoswitching of DASAs, the kinetics of the actinic step is only slightly perturbed. Time-resolved spectroscopy suggests that the same key intermediate  $\mathbf{A}'$  is produced across all solvents studied, giving credibility to the proposed photoswitching mechanism,<sup>[15,16,30]</sup> and showing that in the presented cases the thermal steps are likely rate-limiting. With a full understanding of the actinic step that has now been obtained, it is clear that the focus of future studies will need to shift toward the thermal part of the reaction mechanism to further improve photoswitching and reduce detrimental solvent effects. We foresee immediate application of the lessons learned that make use of the peculiarities of DASAs, not seen in other photoswitches, to inspire the rapidly developing field of visible light molecular photoswitches and beyond.

### Acknowledgements

The authors gratefully acknowledge financial support from Laserlab-Europe (LENS002289, grant no. 654148), the Ministry of Education, Culture and Science (Gravitation program 024.001.035), The Netherlands Organization for Scientific Research (NWO-CW, Top grant to B.L.F., VIDI grant no. 723.014.001 for W.S.), the European Research Council (Advanced Investigator Grant, no. 227897 to B.L.F.) and the Royal Netherlands Academy of Arts and Sciences Science (KNAW). M.M. acknowledges the Czech Science Foundation (project no. 16-01618S), the Ministry of Education, Youth and Sports of the Czech Republic (grant NPU I, LO1305), the Grant Agency of the Slovak Republic (VEGA project No. 1/0737/17) and CMST COST Action CM1405 MOLIM: Molecules In Motion. This research used computational resources of 1) the GENCI-CINES/IDRIS, 2) CCIPL (Centre de Calcul Intensif des Pays de Loire), 3) a local Troy cluster, and 4) the HPCC of the Matej Bel University in Banská Bystrica by using the infrastructure acquired in projects ITMS 26230120002 and 26210120002 supported by the Research and Development Operational Programme funded by the ERDF. The Swiss Study Foundation is acknowledged for a fellowship to M.M.L. We would like to thank Prof. Dr. Wesley R. Browne (University of Groningen, The Netherlands) for fruitful discussions.

### Conflict of interest

The authors declare no conflict of interest.

**Keywords:** donor–acceptor Stenhouse adducts · photoswitches · solvent effects · spectroscopy · visible light

**How to cite:** *Angew. Chem. Int. Ed.* **2018**, *57*, 8063–8068  
*Angew. Chem.* **2018**, *130*, 8195–8200

[1] *Molecular Switches* (Eds.: B. L. Feringa, W. R. Browne), Wiley-VCH, Weinheim, **2011**.

[2] M. M. Russew, S. Hecht, *Adv. Mater.* **2010**, *22*, 3348–3360.

- [3] R. Klajn, *Chem. Soc. Rev.* **2014**, *43*, 148–184.
- [4] H. Tian, J. Zhang, *Photochromic Materials: Preparation, Properties and Applications*, Wiley-VCH, Weinheim, **2016**.
- [5] S. Erbas-Cakmak, D. A. Leigh, C. T. McTernan, A. L. Nussbaumer, *Chem. Rev.* **2015**, *115*, 10081–10206.
- [6] M. Natali, S. Giordani, *Chem. Soc. Rev.* **2012**, *41*, 4010–4029.
- [7] T. Fehrentz, M. Schönberger, D. Trauner, *Angew. Chem. Int. Ed.* **2011**, *50*, 12156–12182; *Angew. Chem.* **2011**, *123*, 12362–12390.
- [8] W. Szymański, J. M. Beierle, H. A. V. Kistemaker, W. A. Velema, B. L. Feringa, *Chem. Rev.* **2013**, *113*, 6114–6178.
- [9] W. A. Velema, W. Szymański, B. L. Feringa, *J. Am. Chem. Soc.* **2014**, *136*, 2178–2191.
- [10] J. Broichhagen, J. A. Frank, D. Trauner, *Acc. Chem. Res.* **2015**, *48*, 1947–1960.
- [11] M. Dong, A. Babalhavaeji, S. Samanta, A. A. Beharry, G. A. Woolley, *Acc. Chem. Res.* **2015**, *48*, 2662–2670.
- [12] M. M. Lerch, M. J. Hansen, G. M. van Dam, W. Szymański, B. L. Feringa, *Angew. Chem. Int. Ed.* **2016**, *55*, 10978–10999; *Angew. Chem.* **2016**, *128*, 11140–11163.
- [13] C. Reichardt, *Chem. Rev.* **1994**, *94*, 2319–2358.
- [14] *Solvents and Solvent Effects in Organic Chemistry* (Eds.: C. Reichardt, T. Welton), Wiley-VCH, Weinheim, **2011**.
- [15] M. M. Lerch, S. J. Wezenberg, W. Szymański, B. L. Feringa, *J. Am. Chem. Soc.* **2016**, *138*, 6344–6347.
- [16] M. Di Donato, M. M. Lerch, A. Lapini, A. D. Laurent, A. Iagatti, L. Bussotti, S. P. Ihrig, M. Medved', D. Jacquemin, W. Szymański, et al., *J. Am. Chem. Soc.* **2017**, *139*, 15596–15599.
- [17] S. Helmy, F. A. Leibfarth, S. Oh, J. E. Poelma, C. J. Hawker, J. Read de Alaniz, *J. Am. Chem. Soc.* **2014**, *136*, 8169–8172.
- [18] S. Helmy, S. Oh, F. A. Leibfarth, C. J. Hawker, J. Read de Alaniz, *J. Org. Chem.* **2014**, *79*, 11316–11329.
- [19] R. Weissleder, V. Ntziachristos, *Nat. Med.* **2003**, *9*, 123–128.
- [20] D. Bléger, S. Hecht, *Angew. Chem. Int. Ed.* **2015**, *54*, 11338–11349; *Angew. Chem.* **2015**, *127*, 11494–11506.
- [21] V. A. Barachevsky, *Rev. J. Chem.* **2017**, *7*, 334–371.
- [22] C. Afonso, R. F. A. Gomes, J. A. S. Coelho, *Chem. Eur. J.* **2018**, <https://doi.org/10.1002/chem.201705851>.
- [23] M. M. Lerch, W. Szymanski, B. L. Feringa, *Chem. Soc. Rev.* **2018**, *47*, 1910–1937.
- [24] J. R. Hemmer, S. O. Poelma, N. Treat, Z. A. Page, N. D. Dolinski, Y. J. Diaz, W. Tomlinson, K. D. Clark, J. P. Hooper, C. Hawker, et al., *J. Am. Chem. Soc.* **2016**, *138*, 13960–13966.
- [25] N. Mallo, P. T. Brown, H. Iranmanesh, T. S. C. MacDonald, M. J. Teusner, J. B. Harper, G. E. Ball, J. E. Beves, *Chem. Commun.* **2016**, *52*, 13576–13579.
- [26] J. N. Bull, E. Carrascosa, N. Mallo, M. S. Scholz, G. da Silva, J. E. Beves, E. J. Bieske, *J. Phys. Chem. Lett.* **2018**, *9*, 665–671.
- [27] E. T. J. Nibbering, H. Fidder, E. Pines, *Annu. Rev. Phys. Chem.* **2005**, *56*, 337–367.
- [28] R. Berera, R. van Grondelle, J. T. M. Kennis, *Photosynth. Res.* **2009**, *101*, 105–118.
- [29] I. H. M. Van Stokkum, D. S. Larsen, R. Van Grondelle, *Biochim. Biophys. Acta Bioenerg.* **2004**, *1657*, 82–104.
- [30] M. M. Lerch, M. Medved', A. Lapini, A. D. Laurent, A. Iagatti, L. Bussotti, W. Szymański, W. J. Buma, P. Foggi, M. Di Donato, et al., *J. Phys. Chem. A* **2018**, *122*, 955–964.

Manuscript received: March 13, 2018  
Version of record online: May 30, 2018